Available online at www.sciencedirect.com
SCIENCE DIRECT®
International Journal of Mass Spectrometry 231 (2004) 189–195
International Journal of Mass Spectrometry
www.elsevier.com/locate/ijms

Influence of the capillary temperature and the source pressure on the internal energy distribution of electrosprayed ions

Valérie Gabelica [a,b,*], Edwin De Pauw [b], Michael Karas [a]

[a] *Institüt für Pharmazeutische Chemie, Johann-Wolfgang Goethe Universität Frankfurt, Marie-Curie Strasse 9-11, D-60439 Frankfurt am Main, Germany*
[b] *Laboratoire de Spectrométrie de Masse, Département de Chimie, Bat. B6c, Université de Liège, B-4000 Liège, Belgium*

Received 23 June 2003; accepted 20 October 2003

Abstract

The internal energy distributions in a heated capillary nano-electrospray source have been determined using the "survival yield" method. At low capillary temperatures, the internal energy distribution is characterized by a low-energy tail, which can be attributed to a fraction of ions not fully desolvated in the heated capillary. This low-energy tais is shown to disappear when the source pressure is increased. This explains why increased source pressure is favorable in the case of highly hydrophilic compounds or non-covalent complexes in order to achieve sufficient desolvation without fragmentation. It is also shown that "high temperature-low voltage" are not equivalent to "low temperature-high voltage" source conditions. These observations are important for fundamental issues as well as for source-CID mass spectral library searching applications.

Keywords: Electrospray; Internal energy; Heated capillary; Pressure effect

1. Introduction

In mass spectrometry, the extent of fragmentation depends on the amount of internal energy received in the source [1]. In electron impact (EI), the content of internal energy is high, leading to electronic and vibrational excitation of the ions. Moreover, as the kinetic energy of the ionizing electrons is precisely fixed (usually 70 eV), and as the source is working at low pressure, the internal energy distribution of the ions is quite reproducible, whatever the instrument used. The EI spectra can therefore be compiled in databases. The application of EI is however restricted to compounds with a sufficient vapor pressure.

Other ionization methods have been developed to allow for the production of gas phase ions from fragile compounds, among which electrospray ionization (ESI) [2,3] and matrix-assisted laser desorption/ionization (MALDI) [4,5] are the most popular. These methods are called "soft" because, when proper experimental conditions are used, intact molecular ions can be produced with minimal fragmentation. Alternatively, fragmentation can be induced on purpose, by changing the instrumental settings of the source. In electrospray, fragmentation is obtained usually by increasing the acceleration voltages in a medium pressure region after the droplet formation. This process is known as in-source collision-induced dissociation, or "source-CID".

The energetic characteristics of ion production and activation by electrospray ionization are much less well defined as compared to electron impact. Nevertheless, different strategies for library generation and library searching of electrospray source-CID mass spectra have been developed [6–12]. In order to perform compound identification by library searching, the experimental and the library spectra must be as similar as possible. It is therefore crucial that "equivalent" source conditions are used for constructing the library and for recording the experimental spectra. "Equivalent" means that both the internal energy distributions and the time scale of the experiment should be as close as possible. In electrospray ionization, spectra strongly differ upon experimental conditions (pressure, acceleration voltage, nature of the solution and of the gas phase). This makes ESI-MS spectra difficult to compare and to reproduce, especially between different instruments. The characterization of the ion internal energy distributions helps to rationalize the differences that may be observed.

* Corresponding author. Tel.: +32-4-3663432; fax: +32-4-3663413.
E-mail address: v.gabelica@ulg.ac.be (V. Gabelica).

1387-3806/$ – see front matter © 2004 Elsevier B.V. All rights reserved.
doi:10.1016/j.ijms.2003.10.010

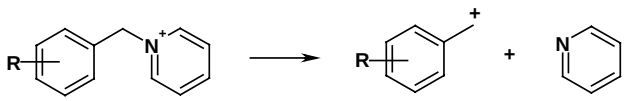

Fig. 1. Structure and fragmentation scheme of the benzylpyridinium cations.

Both Voyksner and Pack [13] and Collette and De Pauw [14] have shown that, upon increasing the orifice-skimmer voltage, the internal energy distributions become wider and are shifted towards higher energies. The nature of the collision gas, for given source settings, can also shift the internal energy distribution of the ions. However, this effect depends greatly on the source design [14–18]. The gas pressure is also a very important parameter, as shown by Schmidt et al. [15], who introduced a gas directly in the capillary-skimmer region of a modified heated capillary source. Increased pressure was found particularly useful in the case of sugars or of non-covalent complexes, in order to facilitate desolvation though preventing unwanted fragmentation. In addition, in their evaluation of the reproducibility of source-CID mass spectral libraries, Bristow et al. [10] noticed that, on some sources, high infusion flow rates resulted in lower fragmentation extent, and attributed this to an increase of the partial pressure in the source.

In the present paper, we investigate the influence of heated capillary temperature and of the source pressure on the shape of the internal energy distributions. These were determined using the previously described "survival yield" method [14,19,20], consisting of measuring the fraction of intact parent ion for a series of benzylpyridinium cations having different threshold fragmentation energies. Those compounds were chosen for their very simple fragmentation mechanism, consisting in the loss of neutral pyridine to give the benzyl cation as the only fragment (Fig. 1). Our results show that the internal energy distributions have a low-energy tail at low capillary temperatures, suggesting that a fraction of the ion population may still be incompletely desolvated at the capillary exit. Upon increasing the source pressure, this low-energy tail disappears, while the high-energy tail of the distribution remains unchanged. The internal energy distribution is therefore narrower, supporting the hypothesis made previously [15].

2. Experimental section

2.1. Instrumentation

We used a Mariner o-TOF instrument (Applied Biosystems, Franmingham, MA) with the electrospray source modified as described previously [15]. Briefly, the nozzle has been replaced by a heated capillary, and an additional needle valve allows some extra gas to be introduced in the region between the capillary and the skimmer. The instrument is equipped with a nano-electrospray source (Protana, now Proxeon Biosystems, Odense, Denmark). For all experiments, the skimmer and the octapole dc voltages were kept constant, at 9.3 and 8.5 V, respectively. This ensures a good ion transfer though minimizing collision-induced dissociation beyond the skimmer. The acceleration in the source is modulated by changing the capillary voltage.

Nano-ESI needles were pulled from borosilicate glass capillaries (Clark Electromedical Instruments, Pangbourne, UK, 1.2-mm o.d., 0.65-mm i.d.) with a micropipet puller (model P-97, Sutter Instrument Co., Novato, CA) to a fine tip with a final inner diameter of approximately 10 μm (open tips) and were coated with gold by means of a sputter coater (model K 550, Emitech, Ashford, UK). Broken capillaries were avoided for reproducibility reasons (see Section 3). Each series of experiments was made with a single capillary, with the needle-capillary voltage difference kept at threshold. This represents an up to 4-h long spray with a single capillary.

2.2. Thermometer molecules

Here we used a slightly different set of molecules than described previously [14,21,22]. A set of all-*para* substituted molecules, listed in Table 1, was used. The advantage is that, as all parent and fragment ions have different masses, all seven molecules can be injected in the same solution. This avoids capillary-to-capillary reproducibility problems (further details below) when comparing the survival yields in order to calculate the internal energy distribution in given instrumental conditions. The first six probe molecules have approximately the same size and number of degrees of freedom, and it will be assumed that they are therefore char-

Table 1
Thermometer molecules used in this study

R	m_{parent} (Da)	$m_{fragment}$ (Da)	DOF[a]	E_0 (eV)[b]	Dilution factor
p-OCH_3	200	121	81	1.508	2
p-CH_3	184	105	78	1.767	6
p-F	188	109	69	1.867	5
p-Cl	204 (^{35}Cl)/206 (^{37}Cl)	125 (^{35}Cl)/127 (^{37}Cl)	69	1.899	10
p-CN	195	116	72	2.097	1
p-NO_2	215	136	75	2.352	5
p-*t*Bu	226	147	105	1.738	200

[a] Number of degrees of freedom of the parent ion.
[b] Calculated with AM1 using Hyperchem (Hypercube Inc.).

acterized by the same internal energy distribution. The energy barriers E_0 (assumed to be equal to the difference between the ΔH_f of the products and the reactant) have been re-calculated by AM1 using Hyperchem 7.0 for Windows (Hypercube, Inc.). The *p*-CN benzylpyridinium cation is a new thermometer molecule which was added to the series to fill the gap between *p*-Cl and *p*-NO_2. The internal energy distributions will be determined with the barriers given in Table 1, with no correction for the kinetic shift. This level of approximation is suitable to investigate the *changes in the shape* of the internal energy distributions, but not for making quantitative determinations of the mean internal energy. It must be noted that the absolute shape of $P(E)$ cannot be determined as the appearance energies ($E_{app} = E_0 + \text{kinetic shift}$) does not vary linearly with the threshold energies (E_0). The *p*-*t*Bu benzylpyridinium cation, which has a higher amount of degrees of freedom, is added to the series to probe the magnitude of the kinetic shift.

All thermometer molecules have a different ionization efficiency in the nano-electrospray conditions used here, depending mainly on the hydrophobicity of the substituent. The ion response increases as follows: *p*-CN < *p*-OCH_3 < *p*-NO_2 ≈ *p*-F < *p*-CH_3 < *p*-Cl ≪ *p*-*t*Bu. In order to have approximately the same parent ion intensities for all thermometer molecules, we had to adapt the dilution factors as shown in Table 1. The solvent used is water/methanol 50/50 (v:v).

3. Results and discussion

3.1. Determination of the shape of internal energy distributions

The "survival yield method" is based on two assumptions. First, all molecules having the same structure and the same number of degrees of freedom have the same internal energy distribution. The first six ions in Table 1 are used for the determination of $P(E)$. The second assumption is that all ions having an internal energy below the dissociation threshold E_0 do not dissociate (are observed as intact parent ion), while all ions having an internal energy above the dissociation threshold do dissociate (are observed as fragments) [14]. The survival yield (SY) of the parent ion (Eq. (1)) is therefore equal to the fraction of the ions that have an internal energy below the threshold, i.e., to the integral below the internal energy distribution $P(E)$ from $E = 0$ to $E = E_0$. If the function SY(E) is the integral of the function $P(E)$, then $P(E)$ (where E is the internal energy) can be found by derivation of SY(E) (where E is the dissociation threshold of the thermometer molecule):

$$\text{SY} = \frac{I(\text{parent})}{I(\text{parent}) + I(\text{fragment})} \quad (1)$$

A typical ESI-MS spectrum of the mixture of thermometer molecules is shown in Fig. 2. For each molecule, the survival yield is calculated using Eq. (1), and plotted as a function of the fragmentation barrier E_0, as shown in Fig. 3a. One more point is added manually, expressing that no parent ion would survive if the fragmentation barrier was equal to zero.

In order not to bias the outcome of the derivation, the rigorous procedure would be to calculate manually the derivate of these few experimental points, i.e., the coordinates of $P(E)$ are given by Eqs. (2) and (3):

$$\text{Ordinate} = \frac{\text{SY}(N+1) - \text{SY}(N)}{E_0(N+1) - E_0(N)} \quad (2)$$

$$\text{Abscissa} = \frac{E_0(N) + E_0(N+1)}{2} \quad (3)$$

Fig. 3 shows a very favorable case for which (i) the survival yields rank correctly with the thresholds (otherwise some of the derivates would be negative) and (ii) the points are well spread between SY = 0 and 1, and therefore the internal energy distribution is well-characterized. However, in most cases, it is more suitable to fit the SY(E) data, and then to derivate the fitting curve to infer $P(E)$, as was done in previous work [14,21]. It must nevertheless be emphasized that the detailed shape of the resulting $P(E)$, especially at the edges, is influenced by the choice of the equation for fitting

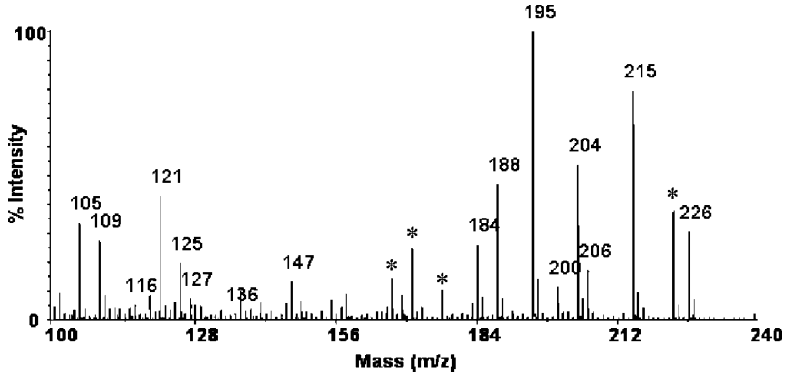

Fig. 2. Typical spectrum of the mixture of thermometer molecules. Nanospray on the Mariner o-TOF instrument, capillary temperature: 60 °C, source pressure: 2.2 mbar, capillary voltage: 200 V. The asterisks indicate peaks due to solvent impurities.

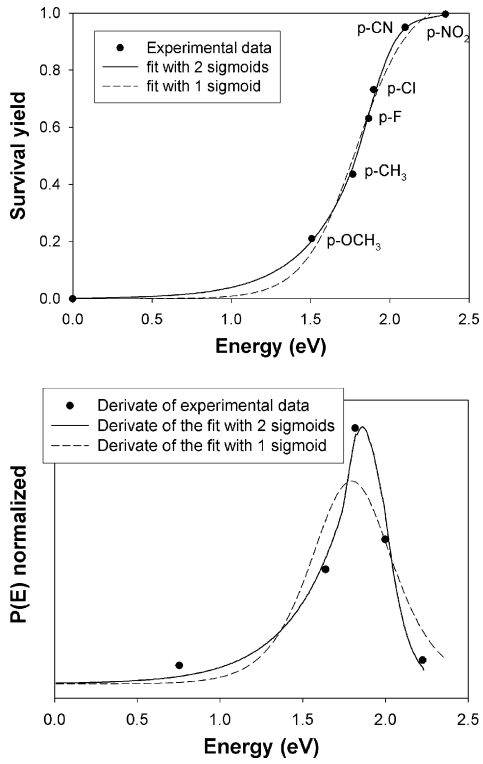

Fig. 3. Influence of the fitting of the survival yields on the shape of the internal energy distribution. Fitting of the datapoints extracted from the spectrum in Fig. 2 by a single sigmoid (dashed line) or by two different sigmoids for the low-energy and the high-energy datapoints (solid line).

the survival yields curve, which is an arbitrary choice. We therefore paid particular attention to this aspect.

Fig. 3 illustrates the procedure we used throughout this study. First the SY(E) data were fitted with a single, symmetrical sigmoid (Eq. (4)):

$$y = \frac{A}{1 + \exp(-(x - x_0)/B)} \quad (4)$$

This is shown by a dashed line in Fig. 3a, and the derivate gives a symmetrical bell-shaped distribution shown in Fig. 3b. However, one can see in Fig. 3a that the single sigmoid does not reflect the actual variation of SY with E. The r^2 of the fitting is only 0.982. When the r^2 for the single sigmoid fit was inferior to 0.995, the fitting was refined by using two sigmoids: one for the first four points, and one for the last four (one point is therefore common to both sigmoids). The two resulting sigmoids were linked at their crossing point, and the resulting curve was smoothed in order to avoid stairs in the derivate. This two sigmoid fitting allows to account for the asymmetry of the internal energy distribution. The result of this procedure is shown by the solid lines in Fig. 3.

3.2. Influence of the capillary temperature

Our first experiments were performed at heated capillary temperatures between 100 and 250 °C, by analogy with the temperatures used previously for sugars and non-covalent

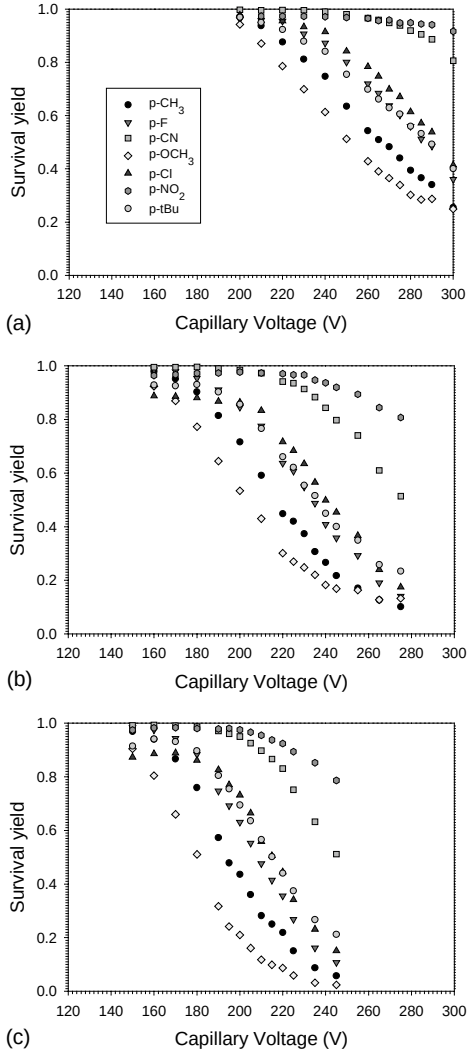

Fig. 4. Survival yields of the thermometer molecules as a function of the capillary voltage at three different capillary temperatures: (a) 50 °C, (b) 55 °C and (c) 60 °C. All data were acquired using the same nanospray capillary. The source pressure was maintained constant at 2.2 mbar.

complexes [15]. The energy distributions obtained with various voltage, capillary temperature and source pressure combinations were all found perfectly symmetrical (fitting with one sigmoid was always satisfactory—data not shown). However, significant departure from a symmetrical distribution could be observed at lower heated capillary temperatures. The fragmentation curves (survival yields as a function of the capillary voltage) at T_{cap} = 50, 55 and 60 °C are shown in Fig. 4.

When the capillary temperature is increased, a lower acceleration voltage is needed in order to achieve a given fragmentation extent. Ions keep a memory of the energy they received in the heated capillary. At higher temperatures, the p-OCH_3 ion is almost completely fragmented at the voltages where the p-CN and p-NO_2 ions start to fragment. Fig. 4 shows that, at low capillary temperatures, it is almost impossible to fragment the ions completely, even at the highest

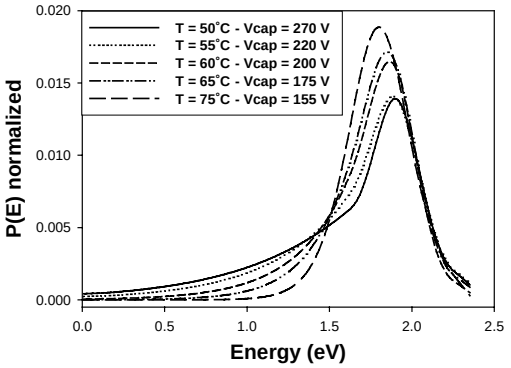

Fig. 5. Comparison between internal energy distributions, in different source conditions giving a survival yield of 0.63 ± 0.01 for the *p*-fluoro-benzylpyridinium cation. The source pressure was maintained constant at 2.2 mbar. From 50 to 65 °C, the SY(*E*) functions had to be fitted using two sigmoids. The curve at 75 °C was satisfactorily fitted using a single sigmoid.

possible capillary-skimmer voltage. As discussed above, the range of experimental conditions where the internal energy distribution can be characterized with confidence is quite narrow. The survival yields have to be well distributed between 0 and 1. Therefore, instead of reporting the internal energy distributions as a function of the increase of the capillary temperature or of the acceleration voltage, we rather compare the internal energy distributions of different sets of source conditions which give the same fragmentation ratio for one of the thermometer molecules. This is shown in Fig. 5. In terms of internal energy distributions, incomplete fragmentation of the most fragile ion (*p*-OCH_3) translates into a low-energy tail (a fraction of the population has not enough energy to fragment) when low capillary temperatures are used. This low-energy tail disappears at capillary temperatures $\geq$75 °C.

In previous work, it was assumed that collisional activation in an electrospray source was virtually equivalent to thermal heating [21–23]. If this were to be true, increasing the acceleration voltages in the source should produce exactly the same effect, in terms of internal energy distribution, as thermally heating the ions in the source, for example in a heated capillary. The present results show that this is not the case in the present instrumental configuration at low capillary temperature. Two effects can account for the fact that "low temperature—high acceleration voltage" conditions are not equivalent to "high temperature—low acceleration voltage" conditions. (i) It has been shown by ion trajectory simulations that the few energetic collisions near the skimmer are those mainly responsible for the internal energy built-up in source-CID [17]. High acceleration voltages could therefore cause a few highly energetic collisions to occur. This would lead however to the appearance of a high-energy tail in the *P*(*E*) in "low temperature—high acceleration" conditions. This is not observed here. (ii) At low capillary temperatures, the ions may not be fully desolvated when entering the capillary-skimmer region of the source. For the fraction of ions which are still solvated (without presuming of the ion formation mechanism), collisional energy is used for the evaporation of the last solvent molecules. Pure collisional activation of the analyte is supposed to occur only when the analyte is yet fully desolvated. This population of partially solvated ions can account for the low-energy tail in the *P*(*E*) observed in "low-temperature—high acceleration" conditions. It must be pointed out that the *P*(*E*) determined here do not necessarily represent the *P*(*E*) of the whole population of ions present in the electrospray droplets, but only of those detected, i.e., those that reached the analyzer as desolvated ions. It must be noted that, despite our efforts, no partially solvated benzylpyridinium ions could ever be detected. At very low capillary temperatures (35–40 °C), only $Na(H_2O)_n^+$ clusters are observed.

The relative position of the fragmentation curve of the *p*-*t*Bu cation allows one to probe the magnitude of the kinetic shift. If the fragmentation time scale was infinitely long, the fragmentation voltage would depend on E_0 only, and the fragmentation curve of *p*-*t*Bu would be between that of *p*-OCH_3 and that of *p*-CH_3. The shorter the fragmentation time scale, the larger the kinetic shift, and the more the fragmentation curve of *p*-*t*Bu will be shifted to higher voltages as compared to the other molecules. It can be seen in Fig. 4 that the kinetic shift is slightly increasing as the capillary temperature increases. We checked by RRKM calculations that the kinetic shift effect alone is unable to account for the different shapes of the fragmentation curves in Fig. 4. However, as the kinetic shift is changing with the source conditions, the exact position of the energy distribution on the energy scale cannot be described quantitatively. Only *changes in the shape* of the *P*(*E*) can be inferred confidently.

The experiments were repeated with several nanospray capillaries. Although the trend shown in Figs. 4 and 5 is reproduced, the fragmentation curves and internal energy distributions shift considerably from one capillary to the other. This is thought to be due to differences in the size of the nano-droplets emitted from the tip of the capillary [24]. This is again consistent with insufficient desolvation as being the origin of the low-energy tail observed in the distributions. Small differences in the initial droplet size would dramatically influence the desolvation extent at the moment of entering the capillary-skimmer region, especially at low capillary temperatures where desolvation is incomplete in the capillary. At high capillary temperatures, the results are much more reproducible from capillary to capillary.

3.3. Influence of the source pressure

Fig. 6 shows the effect of the source pressure on the fragmentation curves of the thermometer molecules at a capillary temperature of 50 °C. The capillary was not the same as the one used for the experiments described in Fig. 4, explaining the different voltage range. As in the case of an in-

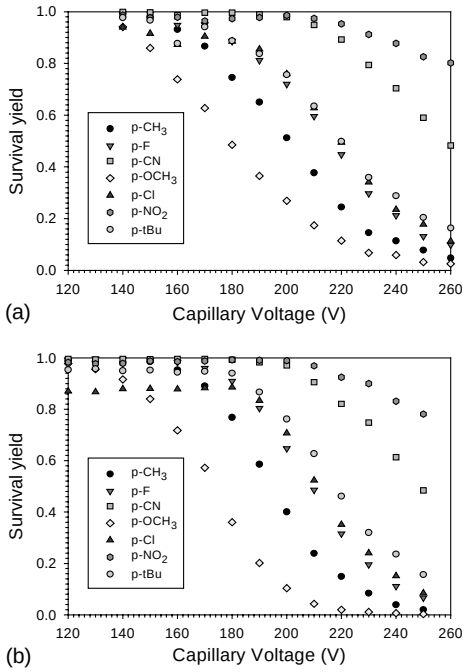

Fig. 6. Survival yields of the thermometer molecules as a function of the capillary voltage at two different pressures: (a) 2.2 mbar and (b) 2.9 mbar. All data were acquired using the same nanospray capillary. The heated capillary temperature was 50 °C.

crease of the source temperature, an increase of the source pressure allows the fragmentation to go to completion for the lowest-stability compound (*p*-OCH_3) at voltages where the fragmentation of *p*-CN and *p*-NO_2 begins. In terms of internal energy distributions (Fig. 7), it means that the low-energy tail of the distribution is suppressed, while the high-energy part remains virtually unchanged. It can also be seen in Fig. 6 that the kinetic shift increases when the source pressure increases, indicating a shorter fragmentation time scale. For this reason, the apparent shift of the mean internal energy when the pressure is increased is actually meaningless, as the internal energy distributions are not corrected for the kinetic shift.

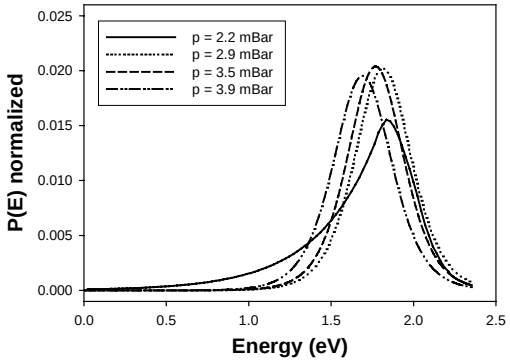

Fig. 7. Influence of the source pressure on the internal energy distributions. Nanospray experiments on the Mariner o-TOF, capillary temperature: 50 °C, capillary voltage: 200 V.

4. Conclusions

The low-energy tail of the internal energy distributions can be attributed to a fraction of the ion population which is not fully desolvated when entering the collision region between the capillary and the skimmer. For ions embedded in a solvent shell or in a droplet, a collision will cause solvent evaporation instead of ion activation. In these conditions, increasing the source pressure increases the number of collisions encountered. There are enough collisions to complete the desolvation step and to further activate the ions. Still, as the mean free path is reduced, the amount of internal energy imparted in the collisions remains small. As a consequence, the internal energy distributions become narrower, as can be seen in Fig. 7. This supports the previous hypothesis that increased source pressure increases the desolvation efficiency while preventing extensive ion activation, which is found useful in the case of sugars (hydrophilic compounds which are therefore hard to desolvate) and non-covalent complexes (which fragment easily upon collisional activation) [15]. Another effect revealed in this study is the increase of the kinetic shift (decrease of the fragmentation time scale) upon increasing the source pressure. In addition purely internal energy effects, this kinetic effect may also contribute to the lower fragmentation observed at increased pressures.

Acknowledgements

VG is a postdoctoral research fellow of the FNRS (Fonds National de la Recherche Scientifique), Belgium, and beneficiated from a Humboldt research fellowship for a 1-year research stay in Germany.

References

[1] K. Vékey, J. Mass Spectrom. 31 (1996) 445.
[2] M. Yamashita, J.B. Fenn, J. Phys. Chem. 88 (1984) 4451.
[3] M. Whitehouse, R.N. Dreyer, M. Yamashita, J.B. Fenn, Anal. Chem. 57 (1985) 675.
[4] M. Karas, D. Bachmann, U. Bahr, F. Hillenkamp, Int. J. Mass Spectrom. Ion Process. 78 (1987) 53.
[5] M. Karas, F. Hillenkamp, Anal. Chem. 60 (1988) 2299.
[6] W. Weinmann, A. Wiedemann, B. Eppinger, M. Renz, M. Svoboda, J. Am. Soc. Mass Spectrom. 10 (1999) 1028.
[7] J.M. Hough, C.A. Haney, R.D. Voyksner, R.D. Bereman, Anal. Chem. 72 (2000) 2265.
[8] W. Weinmann, M. Stoertzel, S. Vogt, J. Wendt, J. Chromatogr. A 926 (2001) 199.
[9] W. Weinmann, M. Stoertzel, S. Vogt, M. Svoboda, A. Schreiber, J. Mass Spectrom. 36 (2001) 1013.
[10] A.W.T. Bristow, W.F. Nichols, K.S. Webb, B. Conway, Rapid Commun. Mass Spectrom. 16 (2002) 2374.
[11] P. Marquet, N. Venisse, E. Lacassie, G. Lachâtre, Analusis 28 (2000) 925.
[12] A.G.A.M. Lips, W. Lameijer, R.H. Fokkens, N.M.M. Nibbering, J. Chromatogr. B 759 (2001) 191.

[13] R.D. Voyksner, T. Pack, Rapid Commun. Mass Spectrom. 5 (1991) 263.
[14] C. Collette, E. De Pauw, Rapid Commun. Mass Spectrom. 12 (1998) 165.
[15] A. Schmidt, U. Bahr, M. Karas, Anal. Chem. 73 (2001) 6040.
[16] B.B. Schneider, D.J. Douglas, D.D.Y. Chen, Rapid Commun. Mass Spectrom. 15 (2001) 249.
[17] A. Hoxha, C. Collette, E. De Pauw, B. Leyh, J. Phys. Chem. A 105 (2001) 7326.
[18] Z. Takats, L. Drahos, G. Schlosser, K. Vékey, Anal. Chem. 74 (2002) 6427.
[19] E. De Pauw, G. Pelzer, J. Marien, P. Natalis, Org. Mass Spectrom. 25 (1990) 103.
[20] F. Derwa, E. De Pauw, P. Natalis, Org. Mass Spectrom. 26 (1991) 117.
[21] C. Collette, L. Drahos, E. De Pauw, K. Vékey, Rapid Commun. Mass Spectrom. 12 (1998) 1673.
[22] L. Drahos, R.M.A. Heeren, C. Collette, E. De Pauw, K. Vékey, J. Mass Spectrom. 34 (1999) 1373.
[23] V. Gabelica, E. De Pauw, J. Mass Spectrom. 36 (2001) 397.
[24] A. Schmidt, M. Karas, T. Dülcks, J. Am. Soc. Mass Spectrom. 14 (2003) 492.